Available online at www.sciencedirect.com
ScienceDirect
Journal of Sound and Vibration 303 (2007) 501–514
JOURNAL OF SOUND AND VIBRATION
www.elsevier.com/locate/jsvi

Control of flexural waves on a beam using a vibration neutraliser: Effects of different attachment configurations

H. Salleh*, M.J. Brennan

Dynamics Group, Institute of Sound and Vibration Research, University of Southampton, Southampton, SO17 1BJ, UK

Received 8 March 2005; received in revised form 28 November 2006; accepted 3 January 2007
Available online 2 April 2007

Abstract

The control of flexural wave motion on a beam using a vibration neutraliser is the subject of this paper. A vibration neutraliser will generally suppress a flexural wave significantly over a narrow frequency band. Although many machines operate at a nominal single frequency, very often there is drift in this frequency. Thus, there is a need for a wide-band vibration neutraliser to attenuate vibration over a reasonably wide frequency range. This paper investigates whether there is any merit in using a particular configuration of neutraliser for such a purpose. The investigation includes a study into the effects of attaching the neutraliser to the beam in different ways. Simple analytical models are developed to aid physical interpretation and facilitate design procedure. Experimental results are also presented to validate the theory.

1. Introduction

There are many practical applications that involve flexural wave motion in beam-like structures found in many engineering sectors such as automotive, aircraft and civil. A simple passive method to control such a wave is to use a vibration neutraliser. For many years vibration neutralisers have not been used explicitly to control waves. The first patented vibration neutraliser was invented by Frahm [1], which consisted of a spring and mass (an undamped absorber). However, the fundamental theory of the vibration neutraliser has been credited to Ormondroyd and Den Hartog [2] when they analysed the device and showed that additional damping increases its effectiveness. Den Hartog [3] subsequently suggested both an optimum damping and stiffness for a neutraliser used to control a single mode of vibration. Snowdon [4] also conducted much of the key work on the application of vibration neutralisers. He considered an optimisation procedure, similar to that used by Den Hartog, for a machine supported by a rubber-like material. He also found that a reasonable vibration reduction could be achieved by using a neutraliser consisting of two springs with one of them in series with a damper [5].

*Corresponding author. Now at: Department of Mechanical Engineering, College of Engineering, Universiti Tenaga Nasional, Km 7 Jalan Kajang-Puchong, 43009 Kajang, Selangor D.E., Malaysia.
E-mail address: hanim@uniten.edu.my (H. Salleh).

0022-460X/$ - see front matter
doi:10.1016/j.jsv.2007.01.025

Ideally, a neutraliser consists of a mass, a spring and a damper. In reality, however, a neutraliser can be made of any resonant system, examples of which are a plate-like system [6,7], a centrifugal pendulum [8] and a cruciform beam arrangement [9,10].

When a neutraliser is used to suppress wave motion on a beam, it has different optimum parameters [11] than those described by Den Hartog. An undamped device will only completely suppress a flexural wave at a single excitation frequency, which here is called the tuned frequency. Such a device can be considered to be a tunable narrow-band vibration control device. In practice, very often there is a drift in the excitation frequency that induces vibration. Thus, there is a need to design a wide-band vibration neutraliser to attenuate vibration over a reasonably wide frequency range. Brennan [11] and Mead [12], studied a single neutraliser that exerts a force only on an infinite beam. However, as mentioned above, this is a narrow-band device. Clark [13] observed that a single neutraliser that exerts a *coupled* force and a moment could improve the bandwidth. This paper follows up on this work and investigates the design of a beam-like neutraliser that exerts an *uncoupled* force and moment to determine whether this can further improve the performance.

The paper is organised into six sections. Following this introduction, Section 2 describes an analytical model for flexural wave transmission on an infinite beam for different neutraliser attachment configurations. In the third section, simple expressions are derived for the tuned frequency and the amount by which an incident flexural wave is suppressed (minimum transmission ratio). The practical implementation of a neutraliser is discussed in the fourth section. In the fifth section some experimental work is discussed and this is followed by some conclusions in the final section.

2. Neutraliser attachment configurations

Four ways in which a neutraliser can be attached to an infinite beam are described in this section. For convenience, the term 'force neutraliser' is used for a neutraliser that exerts a force only to the beam; the term 'moment neutraliser' is used for a neutraliser that exerts a moment only to the beam. The term 'coupled force–moment neutraliser' and 'uncoupled force–moment neutraliser' are used for neutralisers that exert a coupled and an uncoupled force and moment to the beam respectively.

Figs. 1(a–d) show four different types of neutraliser—the force neutraliser, the moment neutraliser, the coupled force–moment and the uncoupled force–moment neutraliser—each attached to an infinite beam. In the figure, m denotes the total mass of the neutraliser, k_s denotes the stiffness of the hysteretically damped spring, η denotes the loss factor, and a denotes the length of the moment arm of the neutraliser, which is assumed to be rigid and massless. If the infinite beam is excited and a propagating wave A_i is incident on a neutraliser, waves are generated downstream of the neutraliser; A_t, which is termed the transmitted propagating wave and A_{nt}, which is termed the transmitted near field wave. The incident wave is also partly reflected upstream as a reflected propagating wave, A_r and a reflected near-field wave, A_{nr}. Throughout this paper $e^{j\omega t}$ time dependence is assumed, but is omitted for clarity. Of particular interest here is the transmission ratio, which is the square of the modulus of the ratio of transmitted propagating wave to the incident wave and is given by

$$\tau = \left|\frac{A_t}{A_i}\right|^2. \tag{1}$$

The transmitted wave is the superposition of the incident wave and the wave generated by the force F, and moment M, applied by the neutraliser and is given by [13,14]

$$A_t = A_i + \frac{1}{4}[-j \quad 1]\begin{bmatrix} \dfrac{F}{EIk_f^3} \\ \dfrac{M}{EIk_f^2} \end{bmatrix} \tag{2}$$

where E, I and k_f are the Young's Modulus, the second moment of area, and the flexural wavenumber of the beam, respectively. The relationships between the force and the moment applied to the beam, and the

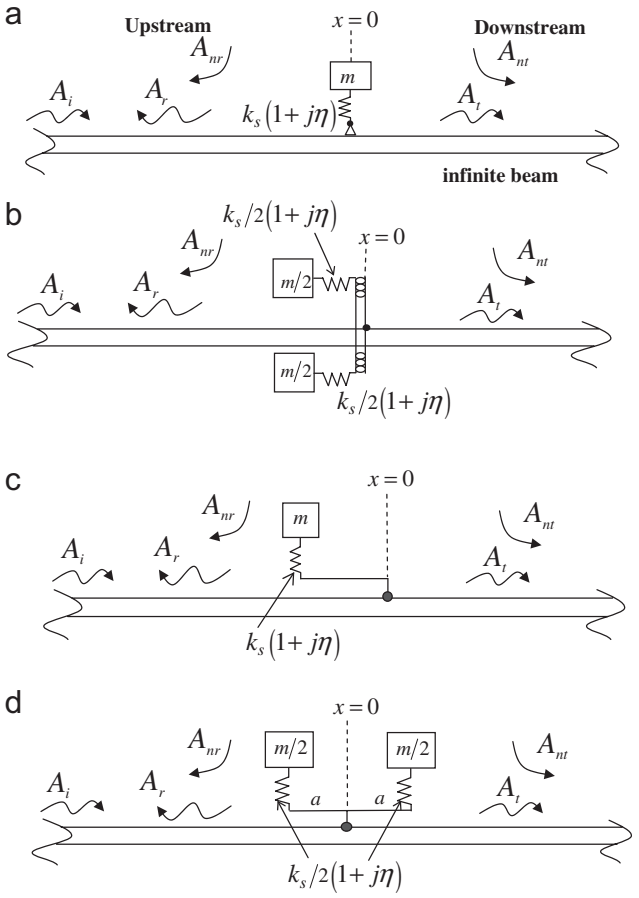

Fig. 1. Various configurations of a neutraliser and hysteretically damped spring attached to an infinite beam: (a) force, (b) moment, (c) coupled force–moment and (d) uncoupled force–moment. The moment arm is assumed to be rigid and massless and has length a.

displacement $w(0)$, and the slope of the beam $w'(0)$ at the point where the neutraliser is attached are given by

$$\begin{bmatrix} \dfrac{F}{EIk_f^3} \\ \dfrac{M}{EIk_f^2} \end{bmatrix} = -\varepsilon_t \begin{bmatrix} 1 & -s \\ -s & s^2 \end{bmatrix} \begin{bmatrix} w(0) \\ \dfrac{w'(0)}{k_f} \end{bmatrix}, \tag{3}$$

where ε_t is the non-dimensional translational dynamic stiffness of the neutraliser given by [10]

$$\varepsilon_t = \frac{K_t}{EIk_f^3} = \frac{\psi(1+j\eta)}{\Omega^2 - 1 - j\eta}, \tag{4}$$

where K_t is the neutraliser translational dynamic stiffness, $\Omega = \omega/\omega_n$ is the ratio of the excitation frequency to the neutraliser undamped natural frequency of translational motion, ψ is the mass ratio, which is the ratio of the neutraliser mass m, to the beam mass of approximately one-sixth of wavelength of the beam, and is given by

$$\psi = \frac{\omega^2 m}{EIk_f^3} = \frac{m}{\rho A\lambda/2\pi}, \tag{5}$$

where λ, ρ and A are the flexural wavelength, the density and the cross sectional area of the beam respectively. It should be noted that the mass ratio is frequency dependent as $\lambda \propto \omega^{0.5}$; s is the ratio of the neutraliser moment arm length a, to approximately one-sixth of a wavelength of the beam and is given by

$$s = \frac{a}{\lambda/2\pi}. \tag{6}$$

The displacement and slope of the beam at the neutraliser attachment point are a function of the incident propagating wave and the force and moment applied by the neutraliser and are given by

$$\begin{bmatrix} w(0) \\ \dfrac{w'(0)}{k_f} \end{bmatrix} = \begin{bmatrix} 1 \\ -j \end{bmatrix} A_i + \frac{1}{4}\begin{bmatrix} -(1+j) & 0 \\ 0 & (1-j) \end{bmatrix} \begin{bmatrix} \dfrac{F}{EIk_f^3} \\ \dfrac{M}{EIk_f^2} \end{bmatrix}. \tag{7}$$

Combining Eqs. (2), (3) and (7) gives the ratio of the transmitted to the incident wave for a neutraliser that applies a coupled force and a moment to the beam.

$$\frac{A_t}{A_i} = 1 - \frac{\varepsilon_t}{4}\begin{bmatrix} -j & 1 \end{bmatrix}\begin{bmatrix} 1 & -s \\ -s & s^2 \end{bmatrix}\left[\begin{bmatrix} 1 & 0 \\ 0 & 1 \end{bmatrix} + \frac{\varepsilon_t}{4}\begin{bmatrix} -(1+j) & 0 \\ 0 & (1-j) \end{bmatrix}\begin{bmatrix} 1 & -s \\ -s & s^2 \end{bmatrix}\right]^{-1}\begin{bmatrix} 1 \\ -j \end{bmatrix} \tag{8}$$

The neutraliser in Fig. 1(a) is attached such that it exerts a force only on the beam, which means that $s = 0$. Applying this condition and substituting for A_t/A_i from Eq. (8) into Eq. (1) results in

$$\tau = \left|1 + \frac{j\varepsilon_t}{4 - \varepsilon_t - j\varepsilon_t}\right|^2. \tag{9}$$

The neutraliser in Fig. 1(b) is attached such that it exerts a moment only to the beam. The moment arm is assumed to be a rigid and massless link. This means that the moment arm ratio matrix $\begin{bmatrix} 1 & -s \\ -s & s^2 \end{bmatrix}$ in Eq. (8) becomes $\begin{bmatrix} 0 & 0 \\ 0 & s^2 \end{bmatrix}$. In this case Eq. (8) combines with Eq. (1) to give

$$\tau = \left|1 + \frac{js^2\varepsilon_t}{4 + s^2\varepsilon_t - js^2\varepsilon_t}\right|^2. \tag{10}$$

The neutraliser in Fig. 1(c) is attached such that it exerts a coupled force and moment to the beam. This means that the Eq. (8) holds, with nonzero terms for all elements of the moment arm ratio matrix. In this case, Eqs. (1) and (8) combine to give the transmission ratio

$$\tau = \left|1 + \frac{-\varepsilon_t - \varepsilon_t s^2 + j(\varepsilon_t + \varepsilon_t s^2)}{4 + 2\varepsilon_t s^2 + j(4 - 2\varepsilon_t)}\right|^2. \tag{11}$$

The neutraliser in Fig. 1(d) is attached such that it exerts an uncoupled force and moment to the beam. This means that the off-diagonal terms of the moment arm ratio matrix are zero. The resulting transmission ratio can be found as before, and is given by

$$\tau = \left|1 + \frac{j\varepsilon_t}{4 - \varepsilon_t - j\varepsilon_t} + \frac{js^2\varepsilon_t}{4 + s^2\varepsilon_t - js^2\varepsilon_t}\right|^2 \tag{12}$$

It can be seen that the transmission ratio is a combination of Eqs. (9) and (10). The second term in Eq. (12) represents the force or translational effect and the third term is due to the moment arm or rotational effect.

Fig. 2 shows the transmission ratios for the four types of neutraliser for $s_n^2 = 0.5$, $\psi_n = 0.5$ and $\eta = 0.001$, which is further discussed in the next section. It should be noted that throughout this paper, the subscript n denotes that the parameter is evaluated at the neutraliser undamped natural frequency of translational motion.

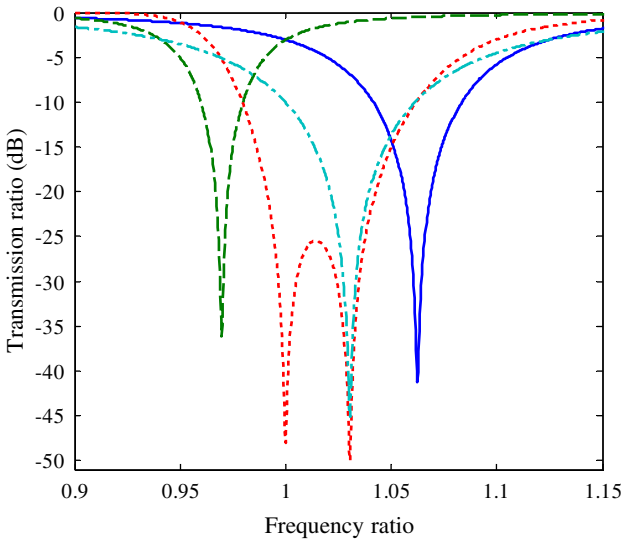

Fig. 2. The transmission ratio for four different configurations of neutraliser attachment as shown in Fig. 1(a–d), $s_n^2 = 0.5$, $\psi_n = 0.5$ and $\eta = 0.001$. Solid line, force neutraliser; dashed line, moment neutraliser; dashed-dotted line, coupled force–moment neutraliser; dotted line, uncoupled force–moment neutraliser.

3. Predicting the tuned frequency and the minimum transmission ratio

The tuned frequency is defined as the frequency at which the transmission ratio is minimum. In Fig. 2, it can be seen that the force neutraliser has a tuned frequency greater than its natural frequency and the moment neutraliser has a tuned frequency less than its natural frequency. The uncoupled force–moment neutraliser has two tuned frequencies, one of which is the same as the tuned frequency for the coupled force–moment neutraliser; the other tuned frequency always occurs at the natural frequency of the neutraliser. In the following subsections approximate expressions for the tuned frequencies and transmission ratios at these frequencies for all four configurations are derived.

3.1. Force neutraliser

Substituting Eq. (4) into Eq. (9), and setting the transmission ratio and loss factor to zero, the tuned frequency, Ω_t, is found to be

$$\Omega_t = \left(1 + \frac{\psi_n}{4}\Omega_t^{1/2}\right)^{1/2}, \tag{13}$$

where ψ_n is the mass ratio evaluated at the natural frequency of the neutraliser. There is no explicit expression for the tuned frequency, but an approximate expression can be derived when $\psi_n/4 \ll 1$, which is

$$\Omega_t \approx 1 + \frac{\psi_n}{8}. \tag{14}$$

This shows that for a force neutraliser, the tuned frequency is always greater than the natural frequency of the neutraliser. In order to reflect a propagating wave with a discontinuity consisting of a translational constraint, a stiffness-like component is required [11]. An infinite beam has a point translational dynamic stiffness characteristic that consists of a mass-like component in parallel with a damper. At the frequency at which an incident propagating wave on the neutraliser is reflected, a local resonance exists between the mass-like component of the beam and the stiffness-like behaviour of the neutraliser. The dynamic stiffness of a neutraliser is mass-like below its natural frequency and stiffness-like above its natural frequency, which explains why the tuned frequency is always greater than the natural frequency for a force neutraliser.

Combining Eqs. (4), (9) and (14) gives the transmission ratio at the tuned frequency [11]

$$\tau_t = \frac{(1 + (\psi_t/4))^2}{(1 + (\psi_t/4\eta))^2}. \tag{15}$$

A practical neutraliser would generally have small mass and damping ratios. Thus, if $\psi_t/4 \ll 1$ and $\psi_t/4\eta \gg 1$, where $\psi_t \approx \psi_n$, then Eq. (15) reduces to

$$\tau_t \approx \left(\frac{4\eta}{\psi_n}\right)^2. \tag{16}$$

This shows that the minimum transmission ratio is proportional to the square of the loss factor and inversely proportional to the square of the mass ratio. Thus, if the mass ratio is increased, the attenuation of an incident propagating wave increases, but the tuned frequency also changes. If the mass ratio is increased by adding to the neutraliser mass, the natural frequency of the neutraliser will decrease, but the difference between the natural frequency and the tuned frequency will increase.

3.2 Moment neutraliser

Substituting Eq. (4). into Eq. (10), setting the transmission ratio and loss factor to zero, the tuned frequency, Ω_t is found to be

$$\Omega_t = \left(1 - \frac{\psi_n}{4} s_n^2 \Omega_t^{3/2}\right)^{1/2}. \tag{17}$$

Again there is no explicit expression for the tuned frequency, but if it is assumed that $\psi_n s_n^2/4 \ll 1$ then the tuned frequency can be approximated by

$$\Omega_t \approx 1 - \frac{\psi_n}{8} s_n^2. \tag{18}$$

Eq. (18) shows that for a moment neutraliser the tuned frequency is always less than the natural frequency of the neutraliser. This is opposite to the force neutraliser where the tuned frequency is always larger than the natural frequency of the neutraliser. This is because a rotational discontinuity needs to present as a mass-like discontinuity. An infinite beam has a point rotational dynamic stiffness that consists of a stiffness-like component in parallel with a damper. At the frequency at which an incident propagating wave on the neutraliser is reflected, a local resonance exists between the stiffness-like component of the beam and the mass-like behaviour of the neutraliser. This explains why the tuned frequency is always less than the natural frequency for a moment neutraliser.

Combining Eqs. (4), (10) and (17) gives the transmission ratio at the tuned frequency

$$\tau_t = \frac{(1 - (\psi_t/4)s_t^2)^2}{(1 + (\psi_t/4\eta)s_t^2(1-\eta))^2 + ((\psi_t/4)s_t^2)^2}. \tag{19}$$

If $\eta \ll 1$, $\psi_t s_t^2/4 \ll 1$ but $\psi_t s_t^2/4\eta \gg 1$, where $\psi_t \approx \psi_n$, $s_t \approx s_n$ then Eq. (19) simplifies to

$$\tau_t \approx \left(\frac{4\eta}{\psi_n s_n^2}\right)^2, \tag{20}$$

which is similar to the expression for the transmission ratio of the force neutraliser given by Eq. (16), but has the additional parameter of the moment arm ratio. This means that, for the same neutraliser mass, for a moment neutraliser to be more effective than the force neutraliser, it is required that $s_n \geqslant 1$ or the moment arm to be greater than about one sixth of a flexural wavelength of the beam at the neutraliser natural frequency.

3.3. Coupled force–moment neutraliser

A neutraliser that exerts a coupled force and moment on the infinite beam as in Fig. 1(c) has a transmission ratio given by Eq. (11). Substituting Eq. (4) into Eq. (11), and setting the transmission ratio and loss factor to zero, the tuned frequency, Ω_t is found to be

$$\Omega_t = \left(1 + \frac{\psi_n \Omega_t^{1/2}}{4}(1 - s_n^2 \Omega_t)\right)^{1/2} \tag{21}$$

It can be seen from Eq. (21) that the tuned frequency depends upon both the mass ratio and the moment arm as expected. If the moment arm is very small then the equation reduces to that for the force neutraliser (Eq. (13)). If the moment arm ratio is large such that $s_n^2 \gg 1$ then Eq. (21) reduces to that for the moment neutraliser (Eq. (17)). Again there is no explicit expression for the tuned frequency, but if it is assumed that $s_n^2 \ll 1$ and that $\psi_n/4 \ll 1$ then Eq. (21) simplifies to

$$\Omega_t \approx 1 + \frac{\psi_n}{8}(1 - s_n^2) \tag{22}$$

The transmission ratio at the tuned frequency is found by combining Eqs. (4), (11) and (21), to give

$$\tau_t = \frac{2(1 + (\psi_t/4)(1 - s_t^2))^2}{(1 + (\psi_t/4\eta)(1 + s_t^2 + 2\eta))^2 + (1 + (\psi_t/4\eta)(1 + s_t^2 - 2s_t^2\eta))^2} \tag{23}$$

If $\eta \ll 1$, $s_t^2 \ll 1$, $\psi_t/4 \ll 1$ and $\psi_t/4\eta \gg 1$, where $\psi_t \approx \psi_n$, $s_t \approx s_n$ then this simplifies to

$$\tau_t \approx \left(\frac{4\eta}{\psi_n(1 + s_n^2)}\right)^2 \tag{24}$$

Eq. (24) shows that, the transmission ratio at the tuned frequency is less than that achievable with either a force or a moment neutraliser; this can also be seen in Fig. 2.

3.4. Uncoupled force–moment neutraliser

A neutraliser attached to an infinite beam via a moment arm, which exerts both a force and moment on the beam, as in Fig. 1(d) has a transmission ratio given by Eq. (12). Substituting Eq. (4) into Eq. (12), and setting the transmission ratio and loss factor to zero, two tuned frequencies can be found. They are

$$\Omega_{t1} = 1, \tag{25a}$$

$$\Omega_{t2} = \left(1 + \frac{\psi_n \Omega_t^{1/2}}{4}(1 - s_n^2 \Omega_t)\right)^{1/2}. \tag{25b}$$

Eq. (25b) is the same as Eq. (21). As can be seen in Fig. 2, one of the tuned frequencies for the uncoupled force–moment neutraliser coincides with the tuned frequency for the coupled force–moment neutraliser. The first tuned frequency occurs because the neutraliser independently applies a large force and a large moment to the beam at the neutraliser resonance frequency, thus, significantly reducing the lateral and rotational motion of the beam at this frequency, and hence reflecting the incident propagating wave.

The transmission ratio at the first tuned frequency, $\Omega_{t1} = 1$, is found as in the previous cases, and given by

$$\tau_{t1} = \frac{\beta}{((4\beta + \psi_t)^2 + \psi_t^2)^2 + ((\beta(4 - 2\psi_t s_t^2) + \psi_t s_t^2)^2 + (\psi_t s_t^2)^2)^2}, \tag{26}$$

where

$$\beta = 16\eta^2\left(\left(1 + \frac{\psi_t}{4}(1 - s_t^2)\right)^2 + (\psi_t(1 - s_t^2))^2\right).$$

If $\eta \ll 1$, $s_t^2 \ll 1$ and $\psi_t \ll 1$, where $\psi_t \approx \psi_n$, $s_t \approx s_n$ the transmission ratio simplifies to

$$\tau_{t1} \approx \left(\frac{2\eta(1-s_n^2)}{\psi_n s_n^2}\right)^2. \tag{27}$$

The transmission ratio at the second tuned frequency is found as before and is given by

$$\tau_{t2} = \frac{\left(\psi_t(1-s_t^2)\left(1+\frac{\psi_t}{2}(1+s_t^2)\right)\right)^2 + \left(4\eta\left(1+\frac{\psi_t}{4}(1-s_t^2)\right)\right)^2}{\left(1+\frac{\psi_t}{4\eta}(1+\eta)\right)^2 + \left(\frac{\psi_t}{4\eta}(s_t^2-\eta)\right)^2 + \left(1+\frac{\psi_t s_t^2}{4\eta}(1-\eta)\right)^2 + \left(\frac{\psi_t}{4\eta}(s_t^2\eta+1)\right)^2}. \tag{28}$$

If $\eta \ll 1$, $s_t^2 \ll 1$, $(\psi_t/4) \ll 1$ and $(\psi_t/4\eta) \gg 1$, where $\psi_t \approx \psi_n$, $s_t \approx s_n$ then this simplifies to

$$\tau_{t2} \approx \left(\frac{4\eta(1-s_n^2)}{\psi_n(1+s_n^4)}\right)^2. \tag{29}$$

It can be seen that, as with the other neutralisers that apply a moment to the beam, the effectiveness of the device at the second tuned frequency is dependent upon both the mass ratio and the length of the moment arm. However, it can also be seen that the moment arm is put to better effect in this device than with the previous two devices. The added advantage of the uncoupled force–moment neutraliser is that it has two tuned frequencies, which means that it is more effective over a wider frequency range.

A further parameter of interest with the uncoupled force–moment neutraliser is the peak transmission ratio between the two minima. This can be seen in Fig. 2. An expression for this can be determined by noting that this local maximum occurs approximately half way between the tuned frequencies, that is when

$$\Omega_p \approx 1 + \frac{\psi_n}{16}(1-s_n^2). \tag{30}$$

This can be combined with Eqs. (4) and (12), and if damping is neglected gives

$$\tau_p \approx \frac{(s_n-1)^2(s_n^4-2s_n^2+1)}{(5s_n^4+2s_n^2+1)(s_n^4+2s_n^2+5)}. \tag{31}$$

This gives a reasonable approximation for the local maximum between $0.1 < s_n^2 < 0.9$ as when $s_n^2 = 0$ and $s_n^2 = 1$ there is only one peak as can be seen by Eq. (25b). Although a value of $s_n^2 > 1$ is possible in principle it is unlikely in practice. It can be readily seen from Eq. (31) that the only factor that affects the local maximum in the response is the non-dimensional length of the moment arm. The minima in the transmission ratio and the maximum response between the minima, given by Eqs. (27), (29) and (31) are plotted in Fig. 3 for $\eta = 0.001$ and $\psi_n = 0.5$. Although both minima in the transmission ratio are dependent on the mass ratio, the moment arm, and the damping in the neutraliser, the ratio of the minima, i.e., the difference in attenuation (in dB) at the tuned frequencies, is only dependent on the length of the moment arm. As the non-dimensional length of the moment arm approaches unity, the two minima merge into one and the local maximum disappears as can be seen in Fig. 3. Thus, the moment arm is an important parameter in controlling the attenuation and the frequency range over which the device is effective.

4. Practical implementation of a neutraliser

A simple design of an uncoupled force–moment neutraliser consists of a beam with a mass attached at each end as shown in Fig. 4. If this device is attached to a beam such that it lies across the beam as shown in Fig. 5a, then it will act as a force neutraliser. If it is rotated through 90° so that it is in-line with the beam as shown in Fig. 5b then it will act as an uncoupled force–moment neutraliser. As these configurations are simple to realise practically, and because there appears to be some advantages in using an uncoupled force–moment neutraliser, they are discussed in detail for the remainder of the paper.

Eq. (9) gives the transmission ratio for the force neutraliser. It is plotted in Fig. 6 for arbitrary properties of the neutraliser and the beam, but with the conditions that, $\psi_n/4 \ll 1$ and $\psi_n/4\eta \gg 1$. The effects that the key

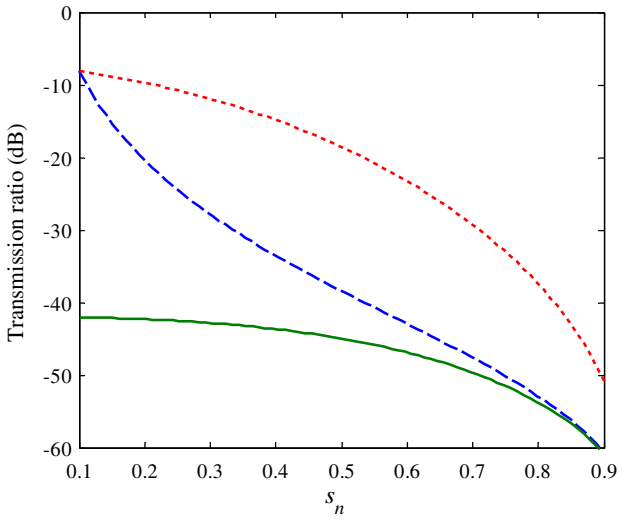

Fig. 3. The relationship between the transmission ratios at the tuned frequencies, the local maximum between the two tuned frequencies, and the non-dimensional moment arm. $\eta = 0.001$ and $\psi_n = 0.5$. Dotted line, τ_p; dashed line, τ_{t1}; solid line, τ_{t2}.

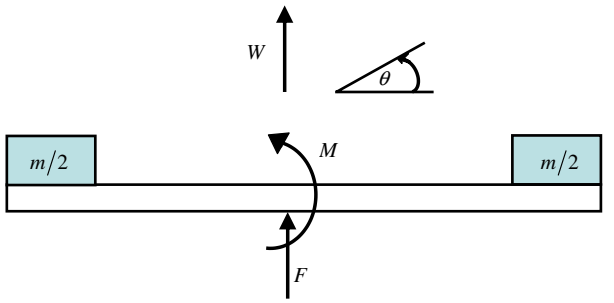

Fig. 4. Sketch of a beam-like neutraliser used in the experimental work. A mass is attached at each end of a beam and the neutraliser is attached to the infinite beam at the centre.

parameters have on the transmission ratio are also shown in the figure. These parameters can be chosen to design a neutraliser to give the required transmission ratio. They can also be used to characterise the neutraliser based on experimental data. Shown in this figure are frequencies Ω_1 and Ω_2, which are the frequencies at which the transmission ratio has a value of -3 dB. The difference between these frequencies is roughly twice the difference between the tuned frequency and the natural frequency of the neutraliser, and is given by $\Omega_2 - \Omega_1 \approx \psi_n/4$. Therefore, this parameter can be used to extract the mass ratio from experimental data. The peak attenuation shown in Fig. 6 can be determined from Eq. (16) and is given by $10\log(\psi_n/4\eta)^2$. Once the mass ratio has been determined, this expression can be used to determine the neutraliser loss factor. This is demonstrated in the next section.

Provided that the masses attached to the neutraliser shown in Fig. 4, are much larger then the mass of the beam from which the neutraliser is fabricated, then Eq. (12) can be used to predict the transmission ratio for this type of neutraliser. It is plotted in Fig. 7 for arbitrary properties of the neutraliser and the beam, but with the conditions that $\psi_n s_n^2/4 \ll 1$ and $\psi_n s_n^2/4\eta \gg 1$. Again, the key parameters are also shown in the figure. It is also possible to extract the parameters from experimental data. The first parameter is s_n which can be determined by noting that $\alpha = 10\log(1/\tau_p)$ and s_n is related to τ_p as in Eq. (31). Once s_n is known, ψ_n can be determined by noting that $\Omega_{t2} - \Omega_{t1} \approx \psi_n(1 - s_n^2)/8$. Finally the expressions for the minima can be used to determine the loss factor, η. Since in practice there will be some differences, the average value should be considered.

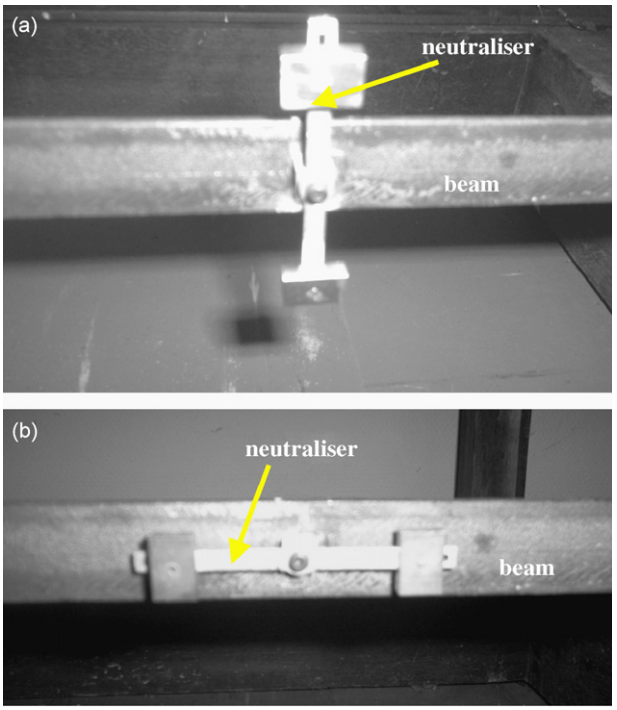

Fig. 5. Attachment of the neutraliser on the beam: (a) force only configuration and (b) uncoupled force–moment configuration.

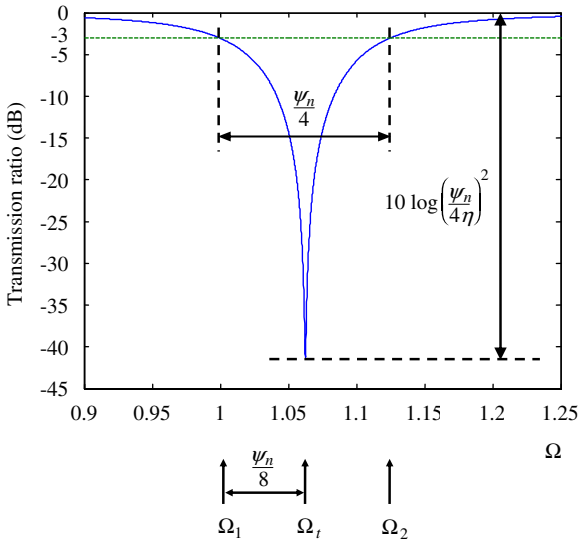

Fig. 6. Transmission ratio for the case where a force only neutraliser is attached to an infinite beam. The properties if the neutraliser and the beam are arbitrary, but $\psi_n/4 \ll 1$ and $\psi_n/4\eta \gg 1$.

5. Experimental work

Experimental work was carried out to validate the performance of the uncoupled force–moment neutraliser and to compare it with the force neutraliser. The experimental set up is shown in Fig. 8. A 4 m beam was used with an anechoic termination fabricated at each end using sand boxes. The properties of the beam are given in Table 1. To calculate the transmission ratio, the flexural waves were decomposed from measurements from

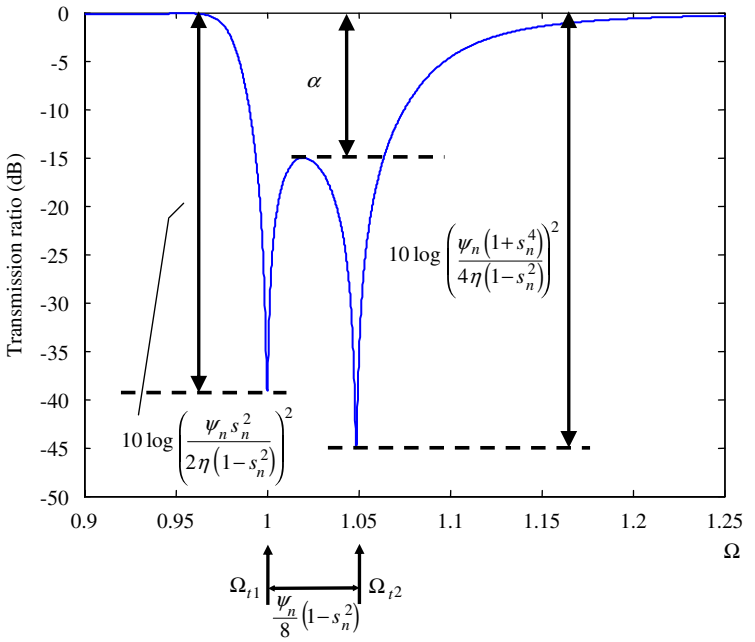

Fig. 7. Transmission ratio for the case where an uncoupled force–moment neutraliser is attached to an infinite beam. The properties if the neutraliser and the beam are arbitrary, but, $\psi_n s_n^2/4 \ll 1$ and $\psi_n s_n^2/4\eta \gg 1$.

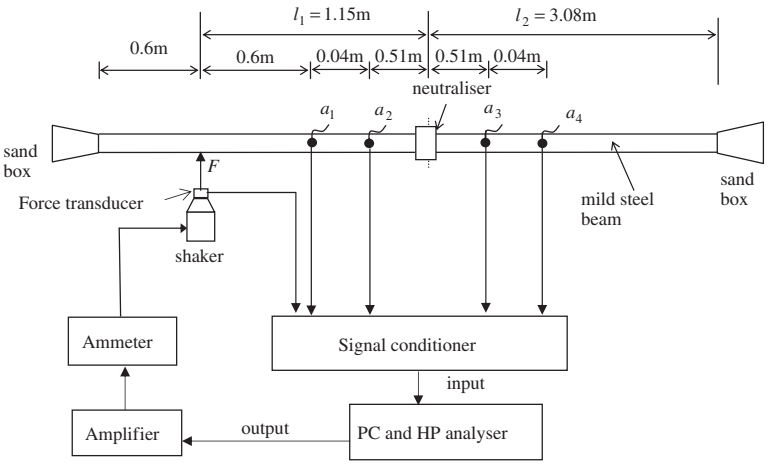

Fig. 8. Experimental set up for measuring the attenuation of a propagating flexural wave on a beam using neutraliser. The neutraliser and accelerometer positions on the beam are also shown.

four accelerometers on the beam (PCB Type 352C22). The force transducer (PCB Type 208C01) was used as a reference signal and the beam was excited with random noise using a Ling Dynamic Systems V201 shaker over the frequency range 50–1600 Hz for all the experiments.

To decompose the waves from acceleration measurements so that the transmission ratio could be calculated, knowledge of the wavenumber is required. Therefore, prior to attaching the neutraliser to the beam, the frequency–wavenumber relationship was estimated. Muggleton et al. [15] used pressure signals to calculate the acoustic wavenumber for a fluid-filled pipe and a similar method was used here using the acceleration signals to calculate the flexural wavenumber of the beam. Three accelerometers were positioned at 1, 1.04 and 1.08 m,

Table 1
Neutraliser and beam dimensions, and material properties

Neutraliser	
Length of aluminium beam between mass centres (m)	53.5e−3
Width of beam (m)	5e−3
Thickness of beam (m)	2e−3
Density of aluminium beam (kg m^{-3})	2720
Young's modulus of aluminium beam (Pa)	70e9
Brass mass at one end (kg)	7.5e−3
Beam	
Length of steel beam (m)	4
Width of beam (m)	2.5e−3
Thickness of beam (m)	3e−3
Density of steel beam (kg m^{-3})	7500
Young's modulus of steel beam (Pa)	210e9

respectively, from the excitation point shown in Fig. 8. The wavenumber was calculated from these measurements using

$$k_f = \frac{\cos^{-1}(0.5((\tilde{a}_1 + \tilde{a}_3)/\tilde{a}_2))}{\Delta}, \tag{32}$$

where $\tilde{a}_1$, $\tilde{a}_2$, $\tilde{a}_3$ are the complex amplitudes of the transfer accelerance at positions 1, 1.04 and 1.08 m, respectively, and Δ is the distance between the sensors. The resulting relationship between the wavenumber and frequency was found to be $k_f = 1.16\sqrt{f}$ using a least squares fit to the measured frequency–wavenumber characteristic. This relationship was also calculated using the data in Table 1, and found to be $k_f = 1.17\sqrt{f}$.

Having determined the wavenumber, two accelerometers were placed upstream and two were placed downstream of the neutraliser as shown in Fig. 8. The accelerometer positions were carefully positioned so that the near-field wave amplitudes were negligible at these locations in the frequency range of 200–500 Hz. It was expected that the following waves would contribute to the overall vibration at the measurement positions; the incidence propagating wave A_i, the transmitted wave A_t, the reflected wave due to the neutraliser A_{r1}, and the reflected wave due to the right-hand side of the sand box A_{r2}. The signal from the force transducer was used as the reference signal. The relationships between these waves and the accelerance measurements are given by [14]

$$\begin{bmatrix} A_i \\ A_{r1} \\ A_t \\ A_{r2} \end{bmatrix} = \frac{F}{-\omega^2} \begin{bmatrix} e^{-jk_f x_1} & e^{jk_f(x_1-l_1)} & 0 & 0 \\ e^{-jk_f x_2} & e^{jk_f(x_2-l_1)} & 0 & 0 \\ 0 & 0 & e^{-jk_f(x_3-l_1)} & e^{jk_f(x_3-l_2)} \\ 0 & 0 & e^{-jk_f(x_4-l_1)} & e^{jk_f(x_4-l_2)} \end{bmatrix}^{-1} \begin{bmatrix} \tilde{a}_1 \\ \tilde{a}_2 \\ \tilde{a}_3 \\ \tilde{a}_4 \end{bmatrix}, \tag{33}$$

where $x_1 = 0.6$ m, $x_2 = 0.64$ m, $x_3 = 1.66$ m and $x_4 = 1.70$ m and l_1, l_2 are shown in Fig. 8. Measurements were taken for both the force neutraliser configuration shown in Fig. 5a and the uncoupled force–moment neutraliser configuration shown in Fig. 5b.

Figs. 9 and 10 show the results for the force and the uncoupled force–moment neutralisers respectively. The experimental data were used to determine the parameters as discussed in Section 4, and the resulting simulations are also plotted in Figs. 9 and 10. For the force neutraliser, the values used for the simulation were $\psi_n = 0.494$, $\eta = 0.021$, whereas for the uncoupled force–moment neutraliser the values used for the simulation were $\psi_n = 0.528$, $\eta = 0.007$ and $s_n = 0.5$.

The characteristics of the neutralisers are summarised in Table 2. It can be seen that the analytical models fit the measured results very well, provided that the parameters used for the simulations are determined from the experimental data. There are some differences between the predicted and measured natural frequencies for both configurations. This is probably due to the fact that it is difficult to estimate the effective length of the

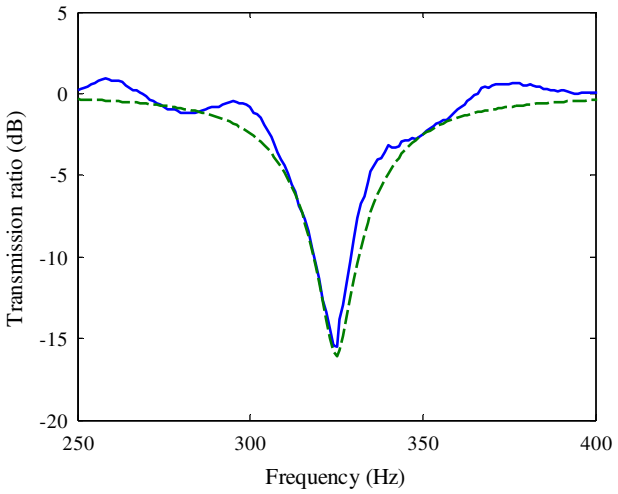

Fig. 9. Experimental result and theoretical prediction of the transmission loss for a force only neutraliser attached to the beam. Solid line, experimental results; dashed line, simulation; $\psi_n = 0.494$, $\eta = 0.021$.

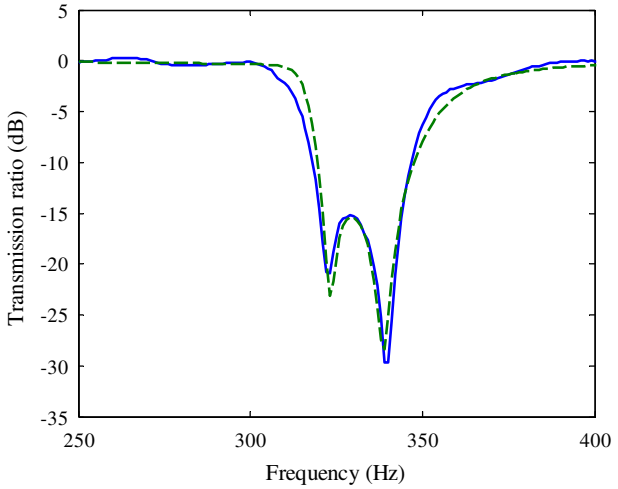

Fig. 10. Experimental result and theoretical prediction of the transmission loss for an uncoupled force–moment neutraliser attached to the beam. Solid line, experimental result; dashed line, simulation; $\psi_n = 0.528$, $\eta = 0.007$ and $s_n = 0.5$.

Table 2
Measured neutraliser characteristics compared with some predictions from the original design

	Estimated from original design	Force neutraliser	Uncoupled force-moment neutraliser
Natural frequency (Hz)	321	306	323
Loss factor, η	—	0.021	0.007
Mass ratio, ψ_n	0.585	0.494	0.528
Moment arm ratio, s_n	0.586	—	0.500
Attenuation at Ω_{t1} (dB)	—	15	22
Attenuation at Ω_{t2} (dB)	—	—	28
3 dB bandwidth (Hz)	—	38	46

beam that contributes to the neutraliser stiffness. The tightness of the connection between the neutraliser and the beam which is assumed to be infinitely rigid can also vary the neutraliser stiffness. Likewise, there is variability between the loss factor for both configurations, and this is probably due to the same reason.

Inspection of Fig. 9 shows that, for the force neutraliser, the attenuation in the transmission ratio at the tuned frequency of the force neutraliser was about 15 dB. Inspection of Fig. 10 shows that, for the uncoupled force–moment neutraliser, the attenuation in the transmission ratio at the two tuned frequencies were 22 and 28 dB, respectively. The −3 dB bandwidth for the two configurations were 38 and 48 Hz, respectively, and the peak in the transmission ratio between the two minima for the uncoupled force–moment neutraliser was about −15 dB. Thus, it can be seen that the uncoupled force–moment neutraliser out-performs the force only neutraliser in all respects.

6. Conclusions

In this paper, four different neutraliser configurations to suppress a propagating flexural wave on a beam have been compared. Two of these, the force-only neutraliser and the uncoupled force moment neutraliser can both be realised simply from a single device, but with different orientation when attached to the beam. These have been studied in detail both analytically and experimentally and have both shown to be effective in attenuating a propagating flexural wave on a beam. However, the uncoupled force–moment neutraliser has proven to be more effective because it can significantly attenuate both translational and rotational motion. Additionally it has two frequencies where it is particularly effective and has a wider bandwidth.

References

[1] H. Frahm, Device for damping vibrations of bodies. US Patent No. 989,958. 1911.
[2] J. Ormondroyd, J.P. Den Hartog, Theory of the dynamic absorber, *Transactions of the ASME* APM 50-7 (1928) 11–22.
[3] J.P. Den Hartog, *Mechanical Vibrations*, McGraw-Hill, New York, 1934 (reprinted by Dover, 1985).
[4] J.C. Snowdon, *Vibration and Shock in Damped Mechanical System*, Wiley, New York, 1968.
[5] J.C. Snowdon, Dynamic vibration absorbers that have increased effectiveness. Transactions of ASME Series B, *Journal of Engineering for Industry* 96 (1974) 940–945.
[6] J.C. Snowdon, Platelike dynamic absorbers. Transactions of ASME series b, *Journal of Engineering for Industry* 97 (1975) 88–93.
[7] J. Clemens, Plate like dynamic absorbers-comparison of measurement and theory, *Journal of Acoustical Society of America* 75 (1984) 638.
[8] M.S. Bakhtiar, S. Shaw, The dynamic response of a centrifugal pendulum vibration absorber with motion limiting stops, *Journal of Sound and Vibration* 126 (1988) 221–235.
[9] J. Snowdon, A. Wolfe, R. Kerlin, The cruciform dynamic absorber, *Journal of Acoustical Society of America* 75 (1984) 1792–1799.
[10] M.J. Brennan, Control of flexural waves on a beam using a tunable vibration neutraliser, *Journal of Sound and Vibration* 222 (3) (1998) 389–407.
[11] M.J. Brennan, Characteristics of a wide-band vibration neutralizer, *Noise Control Engineering Journal* 45 (5) (1997) 201–207.
[12] D.J. Mead, *Passive Vibration Control*, Wiley, Chichester, 1998.
[13] P. Clark, Devices for the Reduction of Pipeline Vibration, Ph.D. Thesis, Institute of Sound and Vibration Research, University of Southampton, UK, 1995.
[14] D.J. Mead, Structural wave motion, in: R.G. White, J.G. Walker (Eds.), *Noise and Vibration*, Ellis Horwood, Chichester, 1982 (Chapter 9).
[15] J.M. Muggleton, M.J. Brennan, P.W. Linford, Axisymmetric wave propagation in fluid-filled pipes: measurements in *in-vacuo* and buried pipes, *Journal of Sound and Vibration* 270 (2004) 171–190.